[1] Dynamic Green Fluorescent Protein Sensors for High-Content Analysis of the Cell Cycle

By SIMON STUBBS and NICK THOMAS

Abstract

We have developed two dynamic sensors that report cell cycle position in living mammalian cells. The sensors use well-characterized components from proteins that are spatially and temporally regulated through the cell cycle. Coupling of these components to Enhanced Green Fluorescent Protein (EGFP) has been used to engineer fusion proteins that report G1/S and G2/M transitions during the cell cycle without perturbing cell cycle progression. Expression of these sensors in stable cell lines allows high content analysis of the effects of drugs and gene knockdown on the cell cycle using automated image analysis to determine cell cycle position and to abstract correlative data from multiplexed sensors and morphological analysis.

Introduction

The cell cycle is one of the most fundamental and complex processes in biology and influences the development, life, and, in cases where it goes wrong, the death of all eukaryotes. Progression of a cell through four phases, G1, S, G2, and M, is exquisitely regulated by a series of checks and balances to ensure that DNA is correctly maintained, replicated, and segregated into daughter cells at division.

The cell cycle and its control mechanisms have been studied extensively for over a century (Nurse, 2000), and significant advances have been made in identifying and describing the role of components and their regulatory mechanisms. Understanding of the cell cycle has progressed to a point where the basic circuitry can be mapped (Kohn, 1999), and ongoing research continues to refine our understanding of the interplay between the players in this game of life (Aleem *et al*., 2005; Cobrinik, 2005; Fu *et al*., 2004; Sherr and Roberts, 2004). Much work remains, and study of the basic molecular mechanisms followed by integration of these mechanisms into a full understanding of cell cycle control and regulation will engage researchers for many years to come (Nurse, 2000a).

The aim of these studies has been twofold: to understand cell cycle control as a key biological process and to gain a greater understanding of the process as an aid in the selection of targets and development of effective drugs for use against the aberrant cell cycle in oncology

METHODS IN ENZYMOLOGY, VOL. 414

0076-6879/06 $35.00
DOI: 10.1016/S0076-6879(06)14001-X

(Carnero, 2002; Gillessen *et al*., 2002; Hamel and Covell, 2002; Sampath and Plunkett, 2001; Stewart *et al*., 2003; Vermeulen *et al*., 2003) and other fields, including cardiovascular (Bicknell *et al*., 2003), neurological (Arendt, 2002) and hepatic (Horie *et al*., 2003) disease, stroke (O'Hare *et al*., 2002), and HIV infection (Galati *et al*., 2002).

Cancer is characterized by deregulated cell cycle control. In contrast to normal cells proliferating only in response to developmental or other mitogenic signals, tumor cell proliferation proceeds automatously. The cell cycle in a cancer cell is not necessarily different from that of a normal cycling cell, but in the cancer cell the accelerator and braking mechanisms that normally control cell cycle progression to give a cell time to repair damaged DNA and to respond to mitogenic stimuli or differentiative inhibition have become decoupled from the cell cycle engine.

In oncology, opportunities for target identification and drug development exist at both G1/S and G2/M transitions as intervention points to target the cell cycle in tumor cells. The G2/M transition has traditionally been the focus of attention, resulting in the development of drugs such as taxol (Hadfield *et al.*, 2003), which interfere with the mechanics of cell division. In more recent programs, new G2/M cell cycle control targets, such as histone deacetylase (Wong *et al*., 2005), aurora kinases (Mortlock *et al*., 2005), Polo-like kinases (PLK) (Blagden and de Bono, 2005), and the G2 checkpoint proteins CHK1 (Li and Zhu, 2002) and CHK2 (Kawabe, 2004), continue to be evaluated and targeted. At the G1/S transition, targets involved in DNA repair and replication, including DNA helicases (Sharma *et al*., 2005), poly(ADP-ribose) polymerase (Jagtap and Szabo, 2005), topoisomerases (Pommier *et al*., 2003), and the MCM complex (Lei, 2005), together with targets controlling G1–S progression, including CDKs (Owa *et al*., 2001), mTOR (Dutcher, 2004), and pRB/E2F (Seville *et al*., 2005), offer alternative approaches to selectively targeting the aberrant cell cycle in cancer cells.

Despite advances in knowledge of the mechanics of the process, the techniques routinely used to study the cell cycle and related events have remained essentially unchanged for many years. Proliferation assays that measure cell numbers (Denizot and Lang, 1986) or radiolabeled thymidine (Graves *et al*., 1997) incorporation can be used to obtain a relatively crude population averaged response to an experimental condition, that is, whether cell growth is stimulated or inhibited, but in asynchronous cells these methods cannot give any indication of which part of the cell cycle is being affected. Higher-resolution methods, including flow cytometry (Smith *et al*., 2000), bromodeoxyuridine incorporation (Humbert *et al*., 1990), and other immunofluorescence techniques (Yuan *et al.*, 2002), allow analysis of cell cycle status at the individual cell level and can be used to determine the distribution of a population of cells around the cell cycle. Despite their

widespread use, all of the aforementioned methods lack the ability to provide a fully dynamic description of the cell cycle in individual cells.

Recent developments in understanding of the control mechanisms of the cell cycle and methods for engineering genetically encoded fluorescent sensors (Tsien, 1998; Zhang *et al*., 2002) have made it possible to design novel cell cycle sensors based on key cell cycle control molecules. When coupled with advances in high-throughput cellular analysis instruments (Lundholt *et al*., 2005; Ramm and Thomas, 2003), these sensors enable high-content analysis of the cell cycle and a high-definition view of the effects of candidate drugs.

Design and Construction of Dynamic Cell Cycle Sensors

Application of fluorescent proteins to cell cycle analysis has enabled significant advances to be made in understanding the timing of molecular events that control the cell cycle. While green fluorescent protein (GFP) fusions with key cell cycle control proteins (Arnaud *et al*., 1998; Huang and Raff, 1999; Raff *et al*., 2002; Weingartner *et al*., 2001; Zeng *et al*., 2000) and other proteins (Kanda *et al*., 1998; Reits *et al*., 1997; Tatebe *et al*., 2001) have provided very significant insights into the molecular mechanics of the cell cycle, expression of cell cycle protein fusions that retain enzyme or structural activity have the potential to perturb the cell cycle and are therefore not suitable as cell cycle sensors (Clute and Pines, 1999).

To provide nonperturbing stealth cell cycle sensors we have developed constructs (Fig. 1) based on the fusion of EGFP to domains isolated from well-characterized cell cycle control and response proteins. The first of these sensors reports on the G1/S transition and the second reports on the G2/M transition.

The G1/S cell cycle phase marker (Fig. 1A and B) is derived from the human homologue of helicase B (HELB), a protein that is essential for G1/S transition (Taneja *et al*., 2002). HELB has been demonstrated to be localized at nuclear foci induced by DNA damage (Gu *et al*., 2004), where the protein operates during G1 to process endogenous DNA damage prior to the G1/S transition. Consistent with the proposed action of HELB, the protein resides in the nucleus during G1 but is predominantly cytoplasmic in S and G2 phase cells. Cell cycle-coordinated nuclear and cytoplasmic residence is controlled by a 131 amino acid C-terminal phosphorylation-dependent subcellular localization control domain (PSLD) containing a nuclear localization sequence that retains the protein in the nucleus in G1 . In late G1 phase, serine residues within the PSLD become phosphorylated by increasing levels of active cyclin E/ Cdk2, resulting in unmasking of a nuclear export sequence leading to protein export to the cytoplasm.

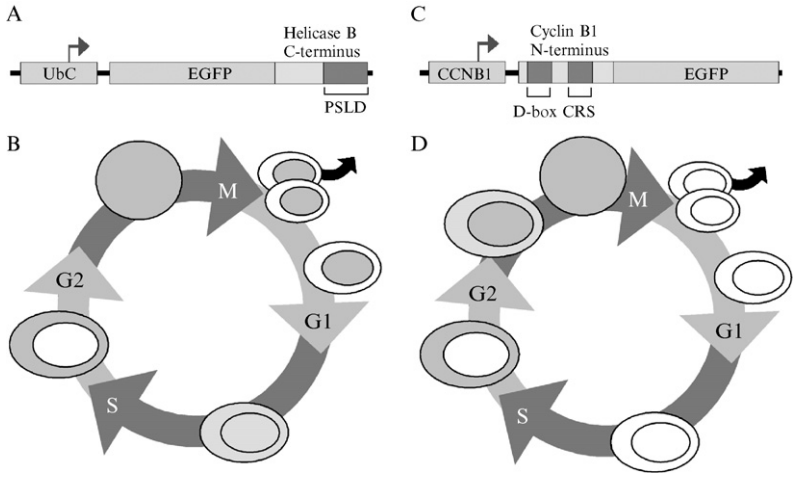

FIG. 1. EGFP cell cycle phase markers. Constitutive expression of the G1/S sensor (A) is achieved via a ubiquitin C (UbC) promoter driving production of a fusion protein between EGFP and the C-terminal region of human DNA helicase B containing a phosphorylation and subcellular localization domain (PSLD). The fluorescent fusion protein localizes to the nucleus in G1 cells (B) and undergoes translocation to the cytoplasm as cells progress through S phase and into G2. Expression of the G2/M sensor (C) is controlled by the cyclin B1 (CCNB1) promoter, which initiates production of the cyclin B1–EGFP fusion protein in late S phase. As cells progress through late S phase into G2, fluorescence increases in the cytoplasm (D) until phosphorylation of the cytoplasmic retention sequence (CRS) causes translocation of the sensor to the nucleus at prophase. At anaphase the sensor is degraded rapidly mediated by the cyclin B1 destruction box (D-box) producing two nonfluorescent daughter cells following mitosis.

The G1/S cell cycle phase marker is a fusion of the PSLD domain of HELB to EGFP, with expression under the control of the human ubiquitin C promoter. The sensor exhibits subcellular localization changes that mimic those of HELB (Figs. 1B and 2B), but does not interfere with cell cycle progression, as the fusion protein lacks the enzymatic and structural domains of the parent protein.

The G2/M cell cycle phase marker (Fig. 1C and D) utilizes functional elements from cyclin B1. Cyclin B1 expression and destruction (Pines, 1999) are tightly regulated and act as a major cell cycle control switch that can be applied to engineering a sensor suitable for following the transition from S phase through G2 into mitosis. The sensor (Thomas, 2003; Thomas and Goodyer, 2003) comprises a fusion of amino acids 1–170 from the amino terminus of cyclin B1 coupled to EGFP, with expression under the control of the cyclin B1 promoter (Hwang *et al.*, 1995). The sensor is switched on in late S phase (Fig. 1D), switched off during mitosis by the

destruction box (D-box) (Clute and Pines, 1999), and, in the intervening period, translocates from the cytoplasm to the nucleus at prophase, regulated by the cytoplasmic retention signal (Hagting *et al.*, 1999). The fusion protein is consequently expressed and degraded in concert with endogenous cyclin B1. Because the fusion protein lacks the C-terminal sequences used in the cyclin B1–CDK interaction, it does not interfere with cell cycle progression as reported previously for a full cyclin B1–GFP fusion protein (Takizawa and Morgan, 2000).

To ensure minimal perturbation of the cell cycle, stable U-2 OS cell lines expressing the G1/S and G2/M sensors were derived through rigorous screening of a large number of clones and selection of single clones that demonstrate minimal levels of EGFP expression compatible with determination of cell cycle status by microscopy and image analysis.

Time-lapse imaging (Fig. 2A) reveals the dynamic behavior of the EGFP sensors through the cell cycle. Both sensors exhibit multiphasic characteristics for EGFP intensity and/or localization (Fig. 2B). The G2/M sensor shows a dramatic drop in intensity following mitosis (0–0.5 h), maintains low fluorescence through G1 (0.5–3 h), and a slow increase in intensity through S phase (3–15 h) followed by a stepped increase in sensor expression through G2 (15–21 h). As cells complete the cell cycle the sensor increases rapidly in intensity as cells pass through prophase (21–22 h) with intensity reaching a maximum at mitosis (23.5 h). The G1/S sensor distribution varies in an opposed fashion. Following mitosis (1.5 h) the sensor is almost entirely restricted to the nucleus and during G1 (1.5–5.5 h) undergoes export to the cytoplasm, resulting in equal sensor distribution between the nucleus and the cytoplasm. Nuclear export continues at a slower rate through to completion of S phase (5.5–14 h), at which time the sensor is predominantly cytoplasmic. Progression through G2 (14–23 h) is accompanied by a slow increase in cytoplasmic intensity as the residual sensor is cleared from the nucleus, followed by a rapid increase in the nuclear/cytoplasmic distribution ratio at mitosis (24 h).

Validation of Sensors

Both G1/S and G2/M sensors have been validated extensively by testing with known cell cycle inhibitors. Analysis of colchicine-induced mitotic blockage in G2/M sensor expressing cells (Fig. 3) confirmed that the sensor reported cell cycle transition and blockage accurately and that quantitative data could be extracted from images acquired by high-throughput microscopy. Treatment of U-2 OS cells expressing the G1/S sensor with a range of cell cycle inhibitors confirmed the cell cycle-related subcellular distribution of the G1/S sensor (Fig. 4) with strong nuclear localization of the sensor in

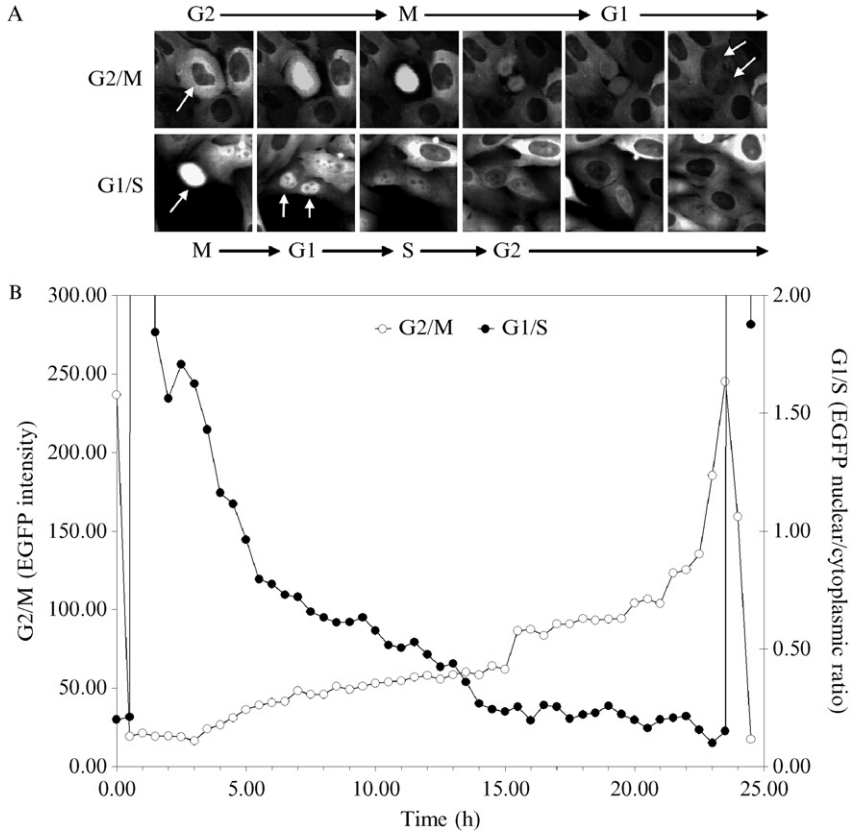

FIG. 2. EGFP cell cycle phase markers. (A) Time-lapse images were acquired on IN Cell Analyzer 3000 of U-2 OS cells stably expressing G2/M (top) and G1/S (bottom) EGFP sensors, and typical cells transitioning the key reporting periods for each cell line are shown. In the G2/M series the central cell in the first frame (arrowed) is in G2 and transitions via prophase (EGFP in nucleus) through mitosis and cytokinesis with destruction of the sensor producing two daughter cells (arrowed) in the final frame with minimal EGFP fluorescence. In the G1/S series the central cell in the first frame (arrowed) is in M and divides to produce two daughter cells with brightly fluorescent nuclei (second frame arrowed), which both transition through S and into G2 with an associated movement of the EGFP sensor from the nucleus to the cytoplasm. (B) Cells from time-lapse images were analyzed for EGFP intensity and subcellular distribution. Typical traces for G1/S (EGFP nuclear/cytoplasmic ratio) and a G2/M (EGFP intensity) sensor expressing cells are shown, each trace starts at mitosis, tracks the sensor output through the cell cycle in a single daughter cell, and finishes at mitosis.

the presence of the G1 blockers roscovitin and olomoucine and distinct cytoplasmic localization in cells exposed to the G2 blockers nocodazole, colcemid, and paclitaxel.

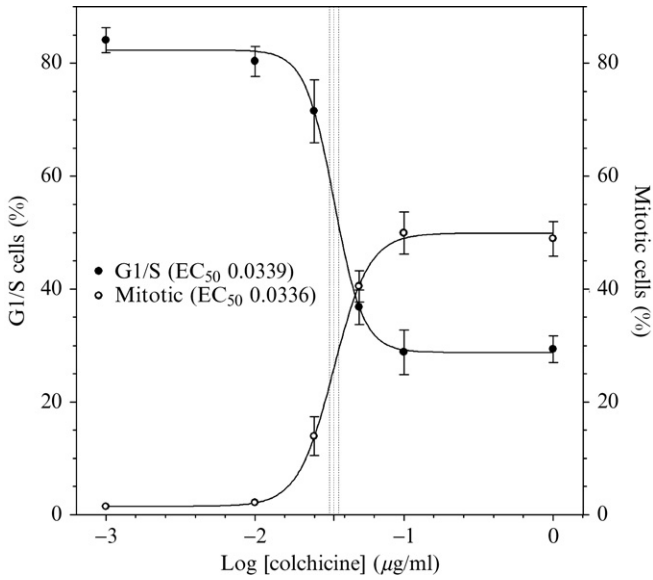

FIG. 3. Cell cycle analysis. G2/M CCPM expressing cells were incubated with increasing concentrations of colchicine and imaged on IN Cell Analyzer 3000. Cells were analyzed for EGFP intensity and distribution using automated image analysis and designated as G1/S, G2, prophase, or mitotic. Dose–response curves are shown for G1/S and M populations with associated EC_{50} derived from the two curves. ($EC_{50} \pm 1$ SD values are shown on the curves by vertical dotted lines).

Coanalysis of the G1/S sensor with BrdU incorporation (Fig. 5) confirmed the indication from time-lapse images (Fig. 2A) that cytoplasmic relocation of this sensor occurs prior to initiation of DNA replication, with BrdU incorporation confined to cells with EGFP nuclear/cytoplasmic ratios indicative of equivalent localization of the sensor in nucleus and cytoplasm following nuclear export of the sensor. Specific changes in the subcellular distribution of the sensor during the cell cycle were further corroborated through comparison with cellular DNA content measured by Hoechst staining. Scatter plot analysis (Fig. 6) of these data shows a U-shaped distribution with cells with a 2*n* genomic DNA complement having a high nuclear to cytoplasmic ratio for the G1S sensor. As cells progress into S phase and DNA content increases, the EGFP nuclear/cytoplasmic ratio decreases, reaching a minimum in cells in G2 (4*n* DNA). Post-G2, the EGFP ratio increases as cells enter mitosis and have a high nuclear to cytoplasmic ratio for the G1/S sensor due to cell rounding.

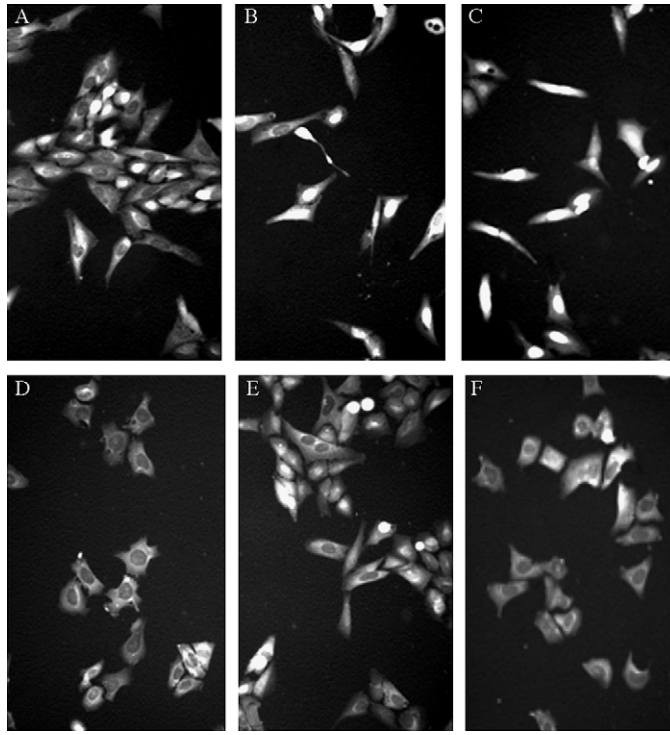

FIG. 4. Cell cycle phase-specific chemical arrest in U-2 OS cells expressing the G1S sensor. Cells were untreated (A) or treated for 24 h with roscovitin (B), olomoucine (C), nocodazole (D), colcemid (E), and paclitaxel (F). Fluorescent, fixed-cell images were acquired on IN Cell Analyzer 1000 using EGFP excitation and emission filters. Cell cycle blocks were confirmed using propidium iodide staining and flow cytometry (data not shown).

In engineering any dynamic sensor it is a critical design requirement that the sensor does not perturb the process it is designed to measure. To evaluate the effect of sensor expression on the cell cycle we compared cell cycle duration and phase distribution by cell proliferation assays and flow cytometry in sensor expressing and parental cells. Cells expressing the G2/M sensor at levels equivalent to endogenous cyclin B1 (7000 copies/cell in G2) (Thomas *et al.*, 2005) showed identical doubling times and cell cycle distributions. Microarray analysis showed no significant differences in expression of cyclins, CDKs, or CDK inhibitors between the two cell types. Similarly, analysis of G1/S sensor expressing cells showed that cell cycle duration and distribution were not affected by sensor expression (data not shown).

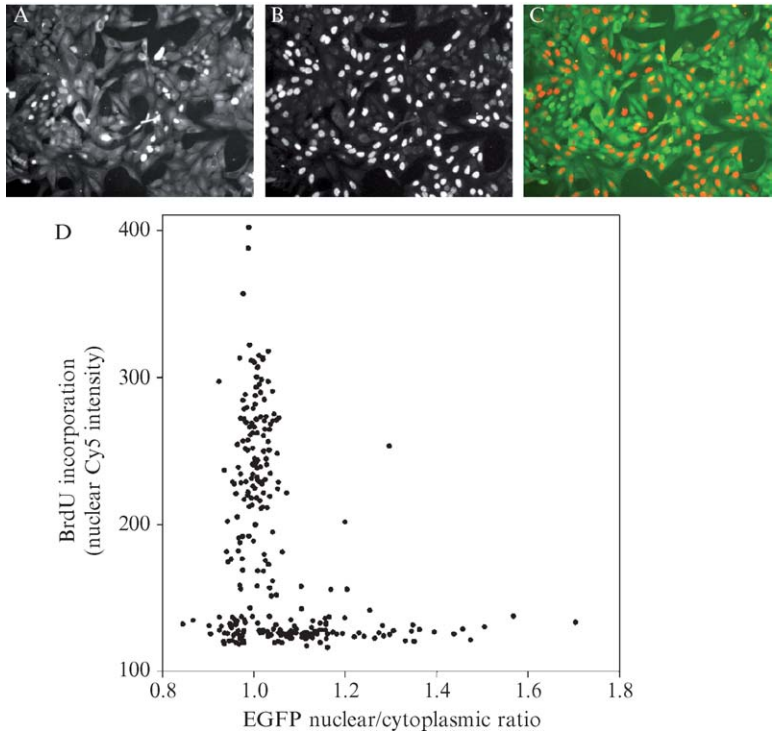

FIG. 5. The G1/S CCPM sensor exhibits subcellular relocation prior to bromodeoxyuridine (BrdU) incorporation. U-2 OS cells stably expressing the G1/S sensor were incubated with BrdU for 1 h and fixed in 4% formaldehyde and imaged on IN Cell Analyzer 1000. (A) EGFP distribution, (B) nuclear BrdU incorporation detected with mouse anti-BrdU/DNAase and Cy5 antimouse antibodies (cell proliferation fluorescence assay, GE Healthcare), and (C) combined false-color image. Images were analyzed with the IN Cell 1000 Analyzer Morphology Analysis Module (GE Healthcare) and to quantify nuclear and cytoplasmic EGFP intensity and BrdU incorporation (D) in each cell. Cells with a predominantly nuclear distribution of the G1S sensor (high Nuc/Cyt ratio) do not exhibit BrdU incorporation, confirming that sensor export from the nucleus occurs before S phase.

Cell Cycle Analysis by Automated High-Throughput Imaging for Drug Profiling and Target Validation

One of the most powerful aspects of high content analysis is the ability to measure dependencies between cellular processes, an area of investigation precluded by population-averaged analyses. The ability to use dynamic sensors for multiplexed analysis of cell cycle status with other probes or with morphological measurements in live or fixed cells now allows study of the interrelationships between cellular events and the cell cycle.

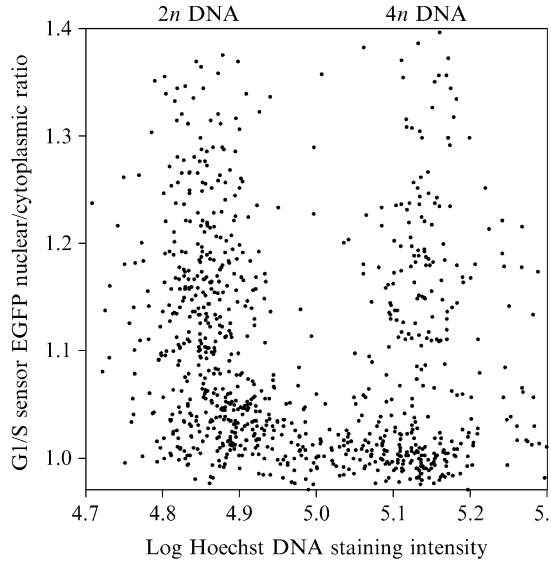

FIG. 6. Sensor localization correlates with cell cycle changes in cellular DNA content. U-2 OS cells expressing the G1/S sensor were fixed and DNA quantitatively stained with Hoechst 33342. Cells were imaged on IN Cell Analyzer 1000 and analyzed for EGFP distribution and DNA content.

Applying these sensors in multiplexed assays using coanalysis of the G2/M or G1/S sensors with measurement of BrdU incorporation and DNA content provide methods to characterize complex drug-induced effects. Figure 7 shows single cell three-parameter data analysis for cells expressing the G1/S sensor incubated in the presence and absence of a putative cell cycle inhibitor (compound A). Data from control cells showed the classical inverted horseshoe pattern typical of flow cytometry analysis of BrdU incorporation versus DNA content (Fig. 7A), with EGFP distribution data providing confirmatory information on cell cycle status. Cells exposed to compound A showed cytokinetic failure with significant numbers of cells exhibiting DNA endoreduplication from 4*n* to 8*n* DNA content after exposure for 24 h (Fig. 7B). G1/S sensor analysis indicated significant numbers of cells in G1 following endoreduplication (large circles on scatter plot). After exposure for 48 h (Fig. 7D) very little BrdU incorporation was evident, with the majority of cells exhibiting polyploid G1 phase arrest. These findings from a fixed cell assay were confirmed by time-lapse fluorescent imaging of cells expressing the G1/S sensor (Fig. 8). Cells treated with compound A showed aberrant cytokinesis with subsequent polyploid arrest in G1.

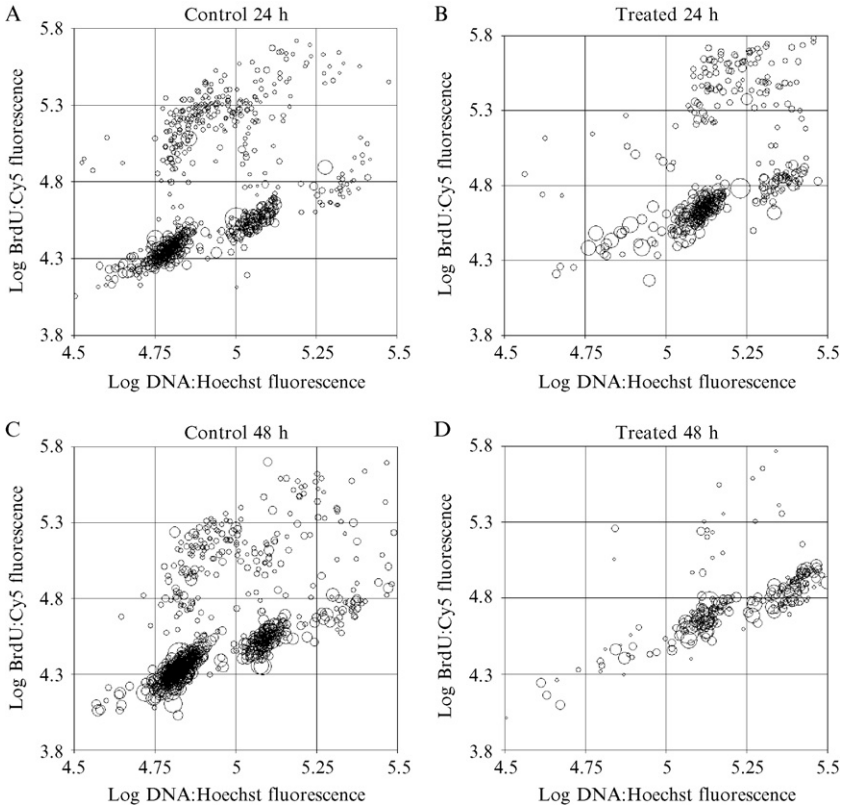

FIG. 7. Multiplexed analysis of DNA endoreduplication in U-2 OS cells stably expressing the G1/S sensor. Cells were grown for 24 h (a and b) or 48 h (c and d) in the presence (b and d) or absence (a and c) of compound A, pulse labeled with BrdU for 1 h, and fixed. Cells were stained with Hoechst 33342 (DNA content) and BrdU detected as described for Fig. 5. Scatter plots show three parameter data for individual cells imaged on the IN Cell Analyzer 1000 and analyzed with the IN Cell 1000 Analyzer Morphology Analysis Module (GE Healthcare). Cellular DNA content is displayed on the *x* axis (log total nuclear blue channel fluorescence from Hoechst:DNA binding), DNA replication as measured by BrdU incorporation on the *y* axis (log total nuclear red fluorescence from anti-BrdU/Cy5 antimouse) and G1/S sensor EGFP distribution (nuclear/cytoplasmic ratio) is proportional to the size of the circles (large circles are G1 phase cells, smaller circles are S phase and G2 phase cells).

We have used the G2/M sensor to multiplex with other fluorescence probes, including cholera toxin (CTX). Analysis of CTX binding to live G2/M CCPM expressing cells (Fig. 9) showed that binding of CTX was restricted to G1 cells confirming previous data obtained from immunofluorescence staining of fixed cells (Majoul *et al.*, 2002). CTX binding occurs through

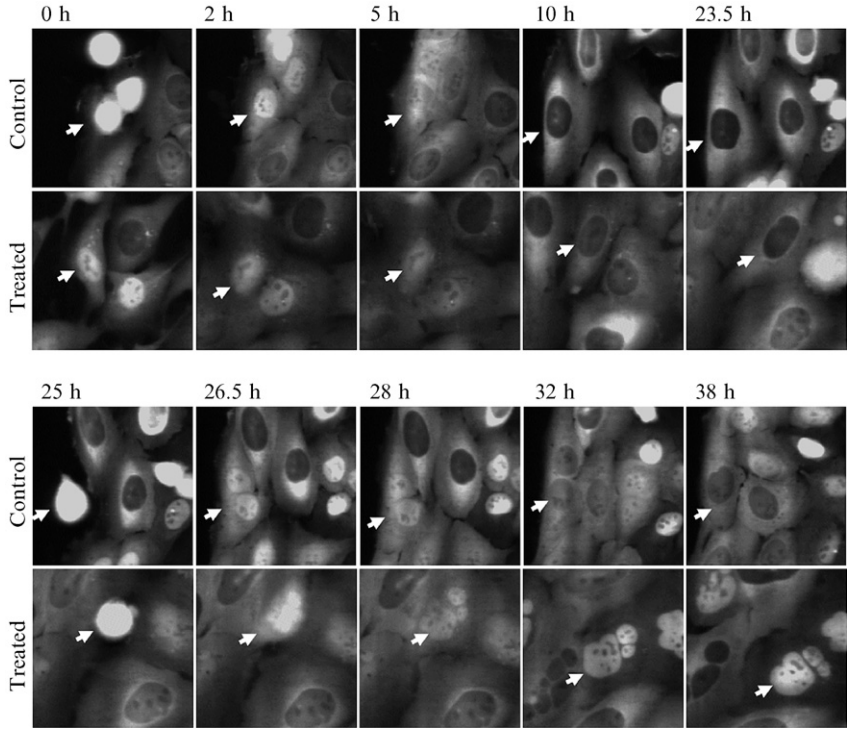

FIG. 8. Inhibition of cytokinesis. U-2 OS cells stably expressing the G1/S sensor were imaged over a 38-h period on IN Cell Analyzer 3000. Arrows highlight representative cells for control populations and populations treated with compound A. Control cells demonstrated a temporally normal cell cycle and entered mitosis around 25 h. Cells in the treated population fail to demonstrate cytokinesis, resulting in large polyploid daughter cells; these cells demonstrate a prolonged period of intense nuclear distribution of the G1/S sensor indicative of polyploid psuedo G1 arrest.

interaction with the plasma membrane ganglioside GM1, which is known to interact with a range of ligands and receptors, including FGF (Rusnati *et al.*, 2002), neuropeptides (Valdes-Gonzalez *et al.*, 2001), the EGF receptor (Miljan *et al.*, 2002), and opiate receptors (Crain and Shen, 1998). The influence of cell cycle-specific expression of a single molecular species over a wide range of biological processes highlights the significant potential for the cell cycle to affect responses in many cell-based assays. By enabling the capture of context-linked events, high content analysis provides a powerful tool for detecting and controlling for cell cycle dependencies in assay data.

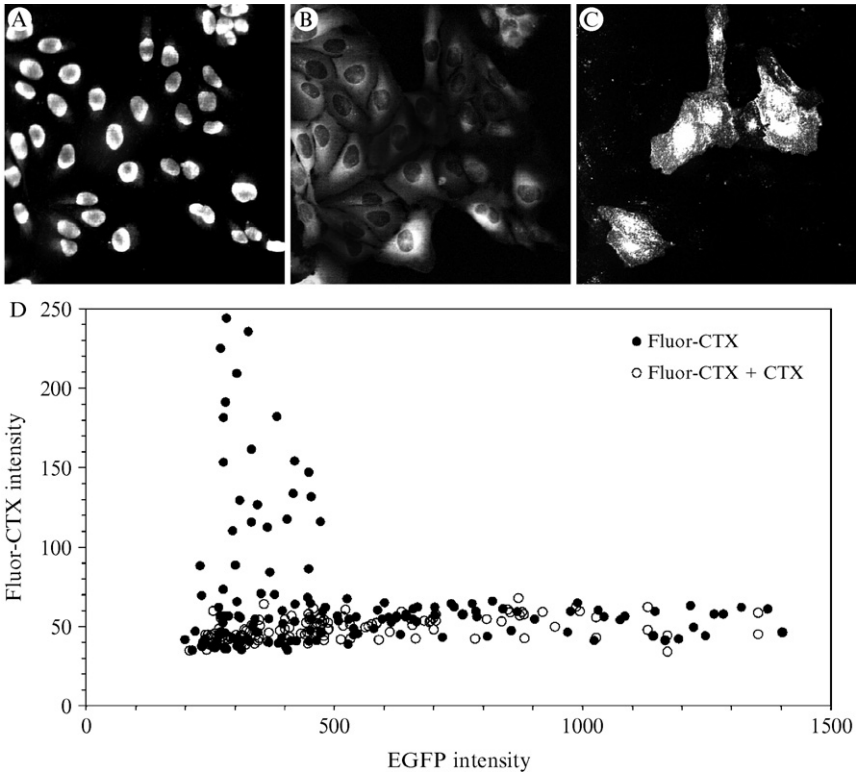

FIG. 9. Multiplexed analysis of ligand binding and cell cycle status. Binding of fluorescently labeled cholera toxin subunit B (CTX-B) to live G2/M CCPM cells was imaged on IN Cell Analyzer3000; (A) Hoechst-stained nuclei (B) EGFP, (C) Alexa-594 labeled CTX-B. (D) EGFP expression and CTX-B binding were determined by image analysis of duplicate wells in the presence and absence of a 100-fold molar excess of unlabeled CTX-B. Specific binding of fluorescent CTX-B is restricted to cells with low EGFP expression, that is, cells in G1.

Recent developments in small interfering RNA (siRNA) techniques for specifically modulating gene expression in a diverse range of cells and organisms have revolutionized the functional analysis of genes and proteins by providing synthetic and virally encoded siRNA methodologies to allow large-scale RNAi screens to be performed in mammalian cells. Combination of siRNA techniques with high content analysis enables study of complex systems by allowing the combination of data from fluorescent cellular sensors with morphological parameters to provide a detailed description of the phenotypic effects of siRNAs in cellular screens.

We have used the G1/S and G2/M sensors in phenotypic screens using two siRNA libraries (Dharmacon) of 120 and 79 siRNA pools directed

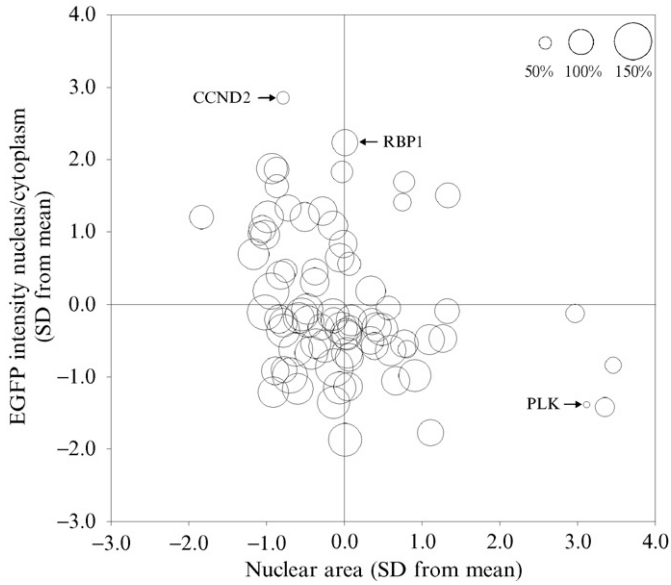

FIG. 10. Multiparameter analysis of siRNA screen in G1/S CCPM. Cells were reverse transfected with a panel of 79 siRNAs directed against cell cycle control and related genes. Cells were imaged on IN Cell Analyzer 3000 and image analysis performed using IN Cell Developer Toolbox to determine cell number, EGFP distribution, and a variety of nuclear morphology parameters. Data for nuclear area, EGFP nuclear/cytoplasmic ratio (high = G1, low = G2), and cell number (circle diameter proportional to cell number as percentage control siRNA) are shown. CCND2, cyclin D2 siRNA; RBP1, retinol-binding protein 1 siRNA; PLK, Polo-like kinase siRNA.

against key cell cycle control genes and other proteins. In screens using the G1/S sensor, a number of siRNAs (cyclin A2, cyclin B1, cyclin B2, cyclin D2, cyclin E1, CDK1, and PLK) produced a significant decrease in cell proliferation (Fig. 10) relative to transfection and siRNA controls. These siRNAs had very similar effects on cell proliferation in parallel screens carried out using the G2/M EGFP sensor (data not shown).

Analysis of the nuclear/cytoplasmic distribution of the EGFP G1/S sensor (Figs. 10 and 11) revealed a number of siRNAs, including cyclin D1, cyclin D2, cyclin E1, cyclin E2, CDK6, CDK7, MDM2, and retinol-binding protein 1 (RBP1), which caused a significant increase in cells in G1. These findings correlate well with the known roles of D- and E-type cyclins and associated CDKs in regulating G1/S transition and with p53-mediated arrest at the G1/S checkpoint via increased p53 activity and consequent inhibition of retinoblastoma protein (RB) phosphorylation.

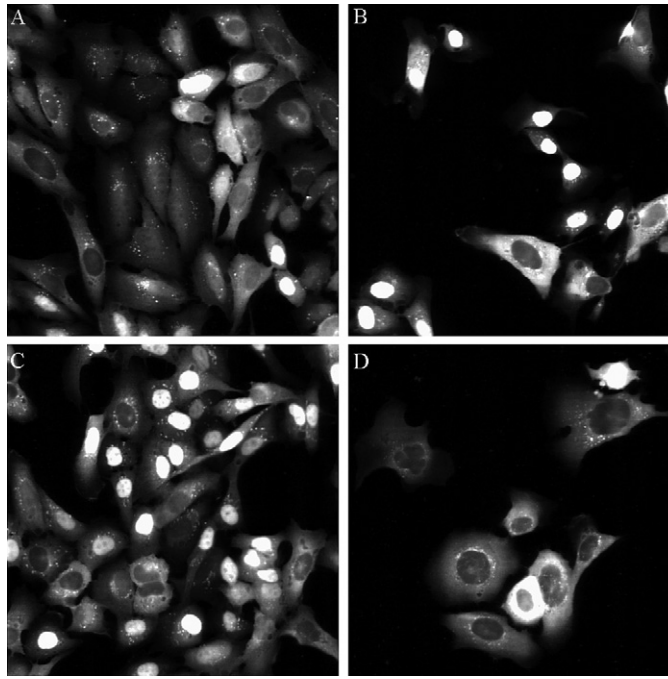

FIG. 11. Effects of siRNAs on cell cycle in G1/S CCPM. Cells were reverse transfected with control (A), cyclin D2 (B), retinal-binding protein (C), and Polo-like kinase (D) siRNAs and EGFP distribution imaged on IN Cell Analyzer 3000.

An interesting and previously unreported observation is the very significant blockage of cells in G1 induced by RBP1 knockdown (Fig. 11C). We postulate that this effect is mediated through intracellular release of retinol and subsequent inhibition of RB phosphorylation mediated through cyclin D and cyclin E and the CDK inhibitors p21 and p27 (Zhang *et al*., 2001; Yu *et al*., 2005).

To further define the effects of siRNAs, images were analyzed using a custom analysis protocol written using IN Cell Developer Toolbox to extract quantitative descriptors of nuclear morphology, including nuclear area (Fig. 10). Of those siRNAs having antiproliferative activity, cyclins A2 and B1, CDK1, and PLK showed significant changes in nuclear morphology. siRNAs producing significant arrest of cells in G1, for example, cyclin D2, MDM2, and RBP1, did not induce significant changes in nuclear morphology. Consequently, abstraction of multiparameter sensor and nonsensor data can be used to characterize siRNA activity into G1 blockers (nuclear EGFP, nuclear morphology unchanged), early G2 blockers (cytoplasmic

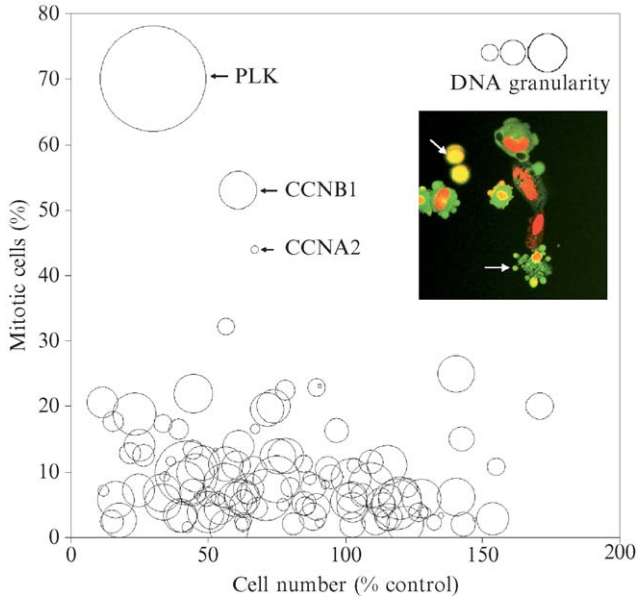

FIG. 12. Multiparameter analysis of siRNA screen in G2/M CCPM. Cells were transfected with a panel of 120 siRNAs directed against cell cycle control and related genes. Cells were imaged on IN Cell Analyzer 1000, and images were converted to IN Cell Analyzer 3000 format and analyzed using cell cycle and nuclear granularity analysis software. Data for cell number, mitotic cells, and DNA granularity (circle diameter proportional to DNA granularity) are shown. PLK, Polo-like kinase siRNA; CCNB1, cyclin B1 siRNA; CCNA2, cyclin A2 siRNA. (Inset) Mitotic and apoptotic cells following treatment with PLK siRNA.

EGFP, nuclear morphology unchanged), and late G2 blockers (cytoplasmic EGFP, significant changes in nuclear morphology).

Similarly, for the screens carried out using the G2/M sensor, applying morphological analysis in addition to cell cycle classification allowed higher resolution characterization of the effects of siRNA knockdown (Fig. 12). Treatment of cells with cyclin A2 siRNA (CCNA2) resulted in a significant accumulation of cells in prophase and mitosis to a similar degree as that observed for cyclin B1 (CCNB1), corresponding with the requirement for cyclin A for G1/S and G2/M transitions. In confirmation of the specificity of siRNA knockdown, cell cycle perturbation was not observed for the germ line functional homologue cyclin A1 (CCNA1), which is not expressed in differentiated U-2OS cells. Morphological analysis of images derived from cells treated with cyclin A2 siRNA revealed a significant increase in nuclear area ($395.3 \pm 173.7\ \mu m^2$) compared to control cells ($219.1 \pm 95.7\ \mu m^2$) and cyclin A1 siRNA-treated cells ($229.8 \pm 98.5\ \mu m^2$).

Knockdown of PLK with siRNA has been shown previously to inhibit cell proliferation, arrest cells in mitosis, and induce apoptosis (Liu and Erikson, 2003). Cell cycle analysis of G2/M sensor cells treated with siRNA directed against PLK showed a dramatic increase in mitotic cells (Fig. 12). Secondary analysis of images for DNA granularity as a measure of apoptotic DNA fragmentation showed a high incidence of apoptosis in PLK siRNA-treated cells. As for the screen described earlier using the G1/S sensor, combining high-content data derived from the same image stack allows subclassification of siRNA knockdown effects, for example, cyclin B1 (G2/M transition) G2/M block, no change in nuclear granularity, cyclin A2 (G1/S and G2/M transition) G2/M block and reduction in nuclear granularity; PLK (G2/M transition) G2/M block and increased nuclear granularity.

Conclusions and Future Directions

Accurate, noninvasive dynamic monitoring of the cell cycle position of individual live cells is of enormous value in the exploration of novel and potentially multiple actions of genes and drug candidates. We believe that cell cycle surveillance sensors of the type described here will enable increasingly sophisticated studies of the mode of action of drugs and chemotherapies in cancer and other diseases by allowing use of a common assay reporter across a range of complementary analysis platforms, including high-throughput imaging and flow cytometry. The use of genetically encoded cell cycle sensors as a measurable phenotype also has significant potential for application in functional genomics. Cellular phenotype screening using forward genetics (Stark and Gudkov, 1999) and large-scale RNAi libraries (Willingham *et al*., 2004) offer complementary approaches to discovery of the role of genes involved in cell cycle regulation and in signaling pathways that are cell cycle dependent.

We are currently developing a range of adenovirally encoded sensors using fluorescent fusion proteins and other sensors (Kendall *et al*., 2006) for use in target validation and lead profiling. Use of adenoviral vectors to deliver encoded cell cycle sensors will enable the development of high content dynamic cell cycle analysis in a wider range of cell types, including primary cells, which offer a more physiologically relevant background for the analysis of gene and drug function than standard transformed laboratory cell lines.

Acknowledgments

The authors thank Hayley Tinkler, Suzanne Hancock, and Mike Kenrick for providing much of the data described here.

References

Aleem, E., Kiyokawa, H., and Kaldis, P. (2005). Cdc2-cyclin E complexes regulate the G1/S phase transition. *Nature Cell Biol.* **7**(8), 831–836.

Arendt, T. (2002). Dysregulation of neuronal differentiation and cell cycle control in Alzheimer's disease. *J. Neural Transm. Suppl.* **62,** 77–85.

Arnaud, L., Pines, J., and Nigg, E. A. (1998). GFP tagging reveals human Polo-like kinase 1 at the kinetochore/centromere region of mitotic chromosomes. *Chromosoma* **107**(6–7), 424–429.

Bicknell, K. A., Surry, E. L., and Brooks, G. (2003). Targeting the cell cycle machinery for the treatment of cardiovascular disease. *J. Pharm. Pharmacol.* **55**(5), 571–591.

Blagden, S., and de Bono, J. (2005). Drugging cell cycle kinases in cancer therapy. *Curr. Drug Targets* **6**(3), 325–335.

Carnero, A. (2002). Targeting the cell cycle for cancer therapy. *Br. J. Cancer* **87,** 129–133.

Clute, P., and Pines, J. (1999). Temporal and spatial control of cyclin B1 destruction in metaphase. *Nature Cell Biol.* **1,** 82–87.

Cobrinik, D. (2005). Pocket proteins and cell cycle control. *Oncogene* **24**(17), 2796–2809.

Crain, S. M., and Shen, K. F. (1998). Modulation of opioid analgesia, tolerance and dependence by Gs-coupled, GM1 ganglioside-regulated opioid receptor functions. *Trends Pharmacol. Sci.* **19**(9), 358–365.

Denizot, F., and Lang, R. (1986). Rapid colorimetric assay for cell growth and survival. Modifications to the tetrazolium dye procedure giving improved sensitivity and reliability. *J. Immunol. Methods* **89**(2), 271–277.

Dutcher, J. P. (2004). Mammalian target of rapamycin (mTOR) inhibitors. *Curr. Oncol. Rep.* **6**(2), 111–115.

Fu, M., Wang, C., Li, Z., Sakamaki, T., and Pestell, R. G. (2004). Cyclin D1: Normal and abnormal functions. *Endocrinology* **145**(12), 5439–5447.

Galati, D., Bocchino, M., Paiardini, M., Cervasi, B., Silvestri, G., and Piedimonte, G. (2002). Cell cycle dysregulation during HIV infection: Perspectives of a target based therapy. *Curr. Drug Targets Immune Endocr. Metabol. Disord.* **2**(1), 53–61.

Gillessen, S., Groettup, M., and Cerny, T. (2002). The proteasome, a new target for cancer therapy. *Onkologie* **25**(6), 534–539.

Graves, R., Davies, R., Brophy, G., O'Beirne, G., and Cook, N. (1997). Noninvasive, real-time method for the examination of thymidine uptake events—application of the method to V-79 cell synchrony studies. *Anal. Biochem.* **248**(2), 251–257.

Gu, J., Xia, X., Yan, P., Liu, H., Podust, V. N., Reynolds, A. B., and Fanning, E. (2004). Cell cycle-dependent regulation of a human DNA helicase that localizes in DNA damage foci. *Mol. Biol. Cell.* **15**(7), 3320–3332.

Hadfield, J. A., Ducki, S., Hirst, N., and McGown, A. T. (2003). Tubulin and microtubules as targets for anticancer drugs. *Prog. Cell Cycle Res.* **5,** 309–325.

Hagting, A., Jackman, M., Simpson, K., and Pines, J. (1999). Translocation of cyclin B1 to the nucleus at prophase requires a phosphorylation-dependent nuclear import signal. *Curr. Biol.* **9**(13), 680–689.

Hamel, E., and Covell, D. G. (2002). Antimitotic peptides and depsipeptides. *Curr. Med. Chem. Anti-Cancer Agents* **2**(1), 19–53.

Horie, T., Sakaida, I., Yokoya, F., Nakajo, M., Sonaka, I., and Okita, K. (2003). L-cysteine administration prevents liver fibrosis by suppressing hepatic stellate cell proliferation and activation. *Biochem. Biophys. Res. Commun.* **305**(1), 94–100.

Huang, J., and Raff, J. W. (1999). The disappearance of cyclin B at the end of mitosis is regulated spatially in Drosophila cells. *EMBO J.* **18**(8), 2184–2195.

Humbert, C., Giroud, F., and Brugal, G. (1990). Detection of S cells and evaluation of DNA denaturation protocols by image cytometry of fluorescent BrdUrd labelling. *Cytometry* **11**(4), 481–489.

Hwang, A., Maity, A., McKenna, W. G., and Muschel, R. J. (1995). Cell cycle-dependent regulation of the cyclin B1 promoter. *J. Biol. Chem.* **270**(47), 28419–28424.

Jagtap, P., and Szabo, C. (2005). Poly(ADP-ribose) polymerase and the therapeutic effects of its inhibitors. *Nature Rev. Drug Discov.* **4**(5), 421–440.

Kanda, T., Sullivan, K. F., and Wahl, G. M. (1998). Histone-GFP fusion protein enables sensitive analysis of chromosome dynamics in living mammalian cells. *Curr. Biol.* **8**(7), 377–385.

Kawabe, T. (2004). G2 checkpoint abrogators as anticancer drugs. *Mol. Cancer Ther.* **3**(4), 513–519.

Kendall, J. M., Ismail, R., and Thomas, N. (2006). Adenoviral sensors for high-content cellular analysis. *Methods Enzymol.* **414** (this volume).

Kohn, K. W. (1999). Molecular interaction map of the mammalian cell cycle control and DNA repair systems. *Mol. Biol. Cell.* **10**(8), 2703–2734.

Lei, M. (2005). The MCM complex: Its role in DNA replication and implications for cancer therapy. *Curr. Cancer Drug Targets* **5**(5), 365–380.

Li, Q., and Zhu, G. D. (2002). Targeting serine/threonine protein kinase B/Akt and cell-cycle checkpoint kinases for treating cancer. *Curr. Top. Med. Chem.* **2**(9), 939–971.

Liu, X., and Erikson, R. L. (2003). Polo-like kinase (Plk)1 depletion induces apoptosis in cancer cells. *Proc. Natl. Acad. Sci. USA* **100**(10), 5789–5794.

Lundholt, B. K., Linde, V., Loechel, F., Pedersen, H. C., Moller, S., Praestegaard, M., Mikkelsen, K., Scudder, K., Bjorn, S. P., Heide, M., Arkhammar, P. O., Terry, R., and Nielsen, S. J. (2005). Identification of Akt pathway inhibitors using redistribution screening on the FLIPR and the IN Cell 3000 Analyzer. *J. Biomol. Screen.* **10**(1), 20–29.

Majoul, I., Schmidt, T., Pomasanova, M., Boutkevich, E., Kozlov, Y., and Soling, H. D. (2002). Differential expression of receptors for Shiga and Cholera toxin is regulated by the cell cycle. *J. Cell Sci.* **115**(Pt. 4), 817–826.

Miljan, E. A., Meuillet, E. J., Mania-Farnell, B., George, D., Yamamoto, H., Simon, H. G., and Bremer, E. G. (2002). Interaction of the extracellular domain of the epidermal growth factor receptor with gangliosides. *J. Biol. Chem.* **277**(12), 10108–10113.

Mortlock, A., Keen, N. J., Jung, F. H., Heron, N. M., Foote, K. M., Wilkinson, R., and Green, S. (2005). Progress in the development of selective inhibitors of Aurora kinases. *Curr. Top Med. Chem.* **5**(2), 199–213.

Nurse, P. (2000). The incredible life and times of biological cells. *Science* **289,** 1711–1716.

Nurse, P. (2000a). A long twentieth century of the cell cycle and beyond. *Cell* **100,** 71–78.

O'Hare, M., Wang, F., and Park, D. S. (2002). Cyclin-dependent kinases as potential targets to improve stroke outcome. *Pharmacol. Ther.* **93**(2–3), 135–143.

Owa, T., Yoshino, H., Yoshimatsu, K., and Nagasu, T. (2001). Cell cycle regulation in the G1 phase: A promising target for the development of new chemotherapeutic anticancer agents. *Curr. Med. Chem.* **12,** 1487–1503.

Pines, J. (1999). Four-dimensional control of the cell cycle. *Nature Cell Biol.* **1**(3), 73–79.

Pommier, Y., Redon, C., Rao, V. A., Seiler, J. A., Sordet, O., Takemura, H., Antony, S., Meng, Z., Liao, Z., Kohlhagen, G., Zhang, H., and Kohn, K. W. (2003). Repair of and checkpoint response to topoisomerase I-mediated DNA damage. *Mutat. Res.* **532**(1–2), 173–203.

Raff, J. W., Jeffers, K., and Huang, J. Y. (2002). The roles of Fzy/Cdc20 and Fzr/Cdh1 in regulating the destruction of cyclin B in space and time. *J. Cell. Biol.* **157**(7), 1139–1149.

Ramm, P., and Thomas, N. (2003). Image-based screening of signal transduction assays. *Sci. STKE* **177,** PE14.

Reits, E. A., Benham, A. M., Plougastel, B., Neefjes, J., and Trowsdale, J. (1997). Dynamics of proteasome distribution in living cells. *EMBO J.* **16**(20), 6087–6094.

Rusnati, M., Urbinati, C., Tanghetti, E., Dell'Era, P., Lortat-Jacob, H., and Presta, M.. (2002). Cell membrane GM1 ganglioside is a functional coreceptor for fibroblast growth factor 2. *Proc. Natl. Acad. Sci. USA* **99**(7), 4367–4372.

Sampath, D., and Plunkett, W. (2001). Design of new anticancer therapies targeting cell cycle checkpoint pathways. *Curr. Opin. Oncol.* **13,** 484–490.

Seville, L. L., Shah, N., Westwell, A. D., and Chan, W. C. (2005). Modulation of pRB/E2F functions in the regulation of cell cycle and in cancer. *Curr. Cancer Drug Targets* **5**(3), 159–170.

Sharma, S., Doherty, K. M., and Brosh, R. M., Jr. (2005). DNA helicases as targets for anti-cancer drugs. *Curr. Med. Chem. Anti-Cancer Agents* **5**(3), 183–199.

Sherr, C. J., and Roberts, J. M. (2004). Living with or without cyclins and cyclin-dependent kinases. *Genes Dev.* **18**(22), 2699–2711.

Smith, P. J., Blunt, N., Wiltshire, M., Hoy, T., Teesdale-Spittle, P., Craven, M. R., Watson, W. B., Amos, W. B., Errington, R. J., and Patterson, L. H. (2000). Characteristics of a novel deep red/infrared fluorescent cell-permeant DNA probe, DRAQ5, in intact human cells analyzed by flow cytometry, confocal and multiphoton microscopy. *Cytometry* **40**(4), 280–291.

Stark, G. R., and Gudkov, A. V. (1999). Forward genetics in mammalian cells: Functional approaches to gene discovery. *Hum. Mol. Genet.* **8**(10), 1925–1938.

Stewart, Z. A., Westfall, M. D., and Pietenpol, J. A. (2003). Cell-cycle dysregulation and anticancer therapy. *Trends Pharmacol. Sci.* **24**(3), 139–145.

Takizawa, C. G., and Morgan, D. O. (2000). Control of mitosis by changes in the subcellular location of cyclin-B1-Cdk1 and Cdc25C. *Curr. Opin. Cell Biol.* **12**(6), 658–665.

Taneja, P., Gu, J., Peng, R., Carrick, R., Uchiumi, F., Ott, R. D., Gustafson, E., Podust, V. N., and Fanning, E. (2002). A dominant-negative mutant of human DNA helicase B blocks the onset of chromosomal DNA replication. *J. Biol. Chem.* **277**(43), 40853–40861.

Tatebe, H., Goshima, G., Takeda, K., Nakagawa, T., Kinoshita, K., and Yanagida, M. (2001). Fission yeast living mitosis visualized by GFP-tagged gene products. *Micron* **32** (1), 67–74.

Thomas, N. (2003). Lighting the circle of life: Fluorescent sensors for covert surveillance of the cell cycle. *Cell Cycle* **2**(6), 545–549.

Thomas, N., and Goodyer, I. (2003). Stealth sensors: Real time monitoring of the cell cycle. *Drug Disc. Today Targets* **2**(1), 26–33.

Thomas, N., Kenrick, M., Giesler, T., Kiser, G., Tinkler, H., and Stubbs, S. (2005). Characterization and gene expression profiling of a stable cell line expressing a cell cycle GFP sensor. *Cell Cycle* **4**(1), 191–195.

Tsien, R. Y. (1998). The green fluorescent protein. *Annu. Rev. Biochem.* **67,** 509–544.

Valdes-Gonzalez, T., Inagawa, J., and Ido, T. (2001). Neuropeptides interact with glycolipid receptors: A surface plasmon resonance study. *Peptides.* **22**(7), 1099–1106.

Vermeulen, K., Van Bockstaele, D. R., and Berneman, Z. N. (2003). The cell cycle: A review of regulation, deregulation and therapeutic targets in cancer. *Cell Prolif.* **36**(3), 131–149.

Weingartner, M., Binarova, P., Drykova, D., Schweighofer, A., David, J. P., Heberle-Bors, E., Doonan, J., and Bogre, L. (2001). Dynamic recruitment of Cdc2 to specific microtubule structures during mitosis. *Plant Cell* **13**(8), 1929–1943.

Willingham, A. T., Deveraux, Q. L., Hampton, G. M., and Aza-Blanc, P. (2004). RNAi and HTS: Exploring cancer by systematic loss-of-function. *Oncogene* **23**(51), 8392–8400.

Wong, C. F., Guminski, A., Saunders, N. A., and Burgess, A. J. (2005). Exploiting novel cell cycle targets in the development of anticancer agents. *Curr. Cancer Drug Targets* **5**(2), 85–102.

Yuan, J., Eckerdt, F., Bereiter-Hahn, J., Kurunci-Csacsko, E., Kaufmann, M., and Strebhardt, K. (2002). Cooperative phosphorylation including the activity of polo-like kinase 1 regulates the subcellular localization of cyclin B1. *Oncogene* **21**(54), 8282–8292.

Yu, Z., Lin, J., Xiao, Y., Han, J., Zhang, X., Jia, H., Tang, Y., and Li, Y. (2005). Induction of cell-cycle arrest by all-trans retinoic acid in mouse embryonic palatal mesenchymal (MEPM) cells. *Toxicol. Sci.* **83**(2), 349–354.

Zeng, Y., Hirano, K., Hirano, M., Nishimura, J., and Kanaide, H. (2000). Minimal requirements for the nuclear localization of p27(Kip1), a cyclin-dependent kinase inhibitor. *Biochem. Biophys. Res. Commun.* **274**(1), 37–42.

Zhang, D., Vuocolo, S., Masciullo, V., Sava, T., Giordano, A., Soprano, D. R., and Soprano, K. J. (2001). Cell cycle genes as targets of retinoid induced ovarian tumor cell growth suppression. *Oncogene* **20**(55), 7935–7944.

Zhang, J., Campbell, R. E., Ting, A. Y., and Tsien, R. Y. (2002). Creating new fluorescent probes for cell biology. *Nature Rev. Mol. Cell. Biol.* **3**(12), 906–918.

[2] High-Content Fluorescence-Based Screening for Epigenetic Modulators

By ELISABETH D. MARTINEZ, ANGIE B. DULL, JOHN A. BEUTLER, and GORDON L. HAGER

Abstract

Epigenetic processes have gained a great amount of attention in recent years, particularly due to the influence they exert on gene transcription. Several human diseases, including cancer, have been linked to aberrant epigenetic pathways. Consequently, the cellular enzymes that mediate epigenetic events, including histone deacetylases and DNA methyltransferases, have become prime molecular targets for therapeutic intervention. The effective and specific chemical inhibition of these activities is a top priority in cancer research and appears to have therapeutic potential. This chapter describes the development of mammalian cell-based fluorescent assays to screen for epigenetic modulators using an innovative combination of approaches. Detailed protocols for the use of the assays in drug screens,

METHODS IN ENZYMOLOGY, VOL. 414

0076-6879/06 $35.00
DOI: 10.1016/S0076-6879(06)14002-1